

Pulsed Laser Ablation in Liquids

Subjects: Nanoscience & Nanotechnology

Contributor: Enza Fazio, Bilal Gökce, Alessandro De Giacomo, Matteo Tommasini, Andrea Lucotti, Paolo Ossi, Marcella Dell'Aglio, Giovanni Gallo, Marco Santoro, Fortunato Neri

Laser synthesis emerges as a suitable technique to produce ligand-free nanoparticles, alloys and functionalized nanomaterials for catalysis, imaging, biomedicine, energy and environmental applications. In the last decade, laser ablation and nanoparticle generation in liquids has proven to be a unique and efficient technique to generate, excite, fragment and conjugate a large variety of nanostructures in a scalable and clean way.

Keywords: colloids ; plasmonics ; sensing ; biomedicine ; catalysis ; pollutants ; pulsed laser ablation in liquids

1. Introduction

The intrinsic properties of nanoparticles (NPs), possibly combined with other materials, disclose many applications where one can achieve miniaturization (e.g., of electronic equipment), weight reduction (as a result of an increased material efficiency) and/or improved functionalities of materials (e.g., higher durability, conductivity, thermal stability, solubility, reduced friction, selective molecular detection) ^{[1][2]}. The remarkable size-tunable properties of nanomaterials produced by laser-matter interaction (e.g., size distribution, agglomeration state/dispersion, crystal structure, surface area and porosity, surface charge, shape/morphology, dissolution/solubility) make them a hot research topic in material science, with far-reaching applications, ranging from quantum computers to cures for cancer ^{[3][4]}.

Bottom-up and top-down procedures are the two approaches used for the synthesis of nanomaterials ^[5]. The first include the miniaturization of materials and components (up to the atomic level) with subsequent self-assembling that leads to the formation of nanostructures. Typical examples are the formation of quantum dots during epitaxial growth, or the production of NPs as colloidal dispersions by chemical approaches ^[6]. Instead, top-down approaches use macroscopic starting structures that are externally controlled by the processing down to nanostructures. Typical examples are etching (controlled by masks), ball milling, metal-organic vapor phase epitaxy and the application of severe plastic deformations ^[7].

Many papers are available in the literature on laser interaction with hard, soft and smart materials, targeting future applications in the fields of energy production (nano-energy) and biomedicine ^[8], as well as recent progress in the understanding of the fundamental mechanisms involved in laser processing ^{[9][10]}. Such laser techniques are interesting in many regards, as they enable the processing of photovoltaic cells ^[11], thermoelectric materials and devices ^[12], micro and nanosystems for energy storage and conversion ^{[13][14]}, biodegradable and biocompatible NPs for food packaging ^[15] as well as vectors for drug and gene delivery ^{[16][17]}. The interest towards pure and electrostatically stabilized nanocolloids is well recognized ^{[18][19][20][21][22][23]}. Although nanotechnologies and nanomaterials have much potential to introduce innovative products and production processes, they are facing major challenges in being cost-effective in the production stage.

Laser synthesis of colloids, powered by robust, high-power lasers, appears to be a key enabling process that is chemically clean and environmentally friendly, and appealing ^{[24][25]} for industrial manufacturing of functional nanomaterials while being useful in many different areas, such as: hydrogen generation ^[17], hydrogen storage ^[26], heterogeneous catalysis using colloidal high-entropy alloy NPs ^{[27][28]}, anticancer ^[29] and antimicrobial ^[30] research, drug monitoring ^[31], additive manufacturing applications ^{[32][33]}, and nonlinear nanophotonics ^[34]. In addition, NPs prepared by the Laser Ablation in Liquids (LAL) have been recently used for various and unique applications like friction reduction ^[35], solar nanofluids ^[36] ^[37], optical limiting devices ^{[38][39]} and so on.

The generation of NPs with LAL still has some challenging aspects, such as the fabrication of NPs with a specific size and shape, the reduction of polydispersity and the increase of productivity ^[40]. Despite some unsolved problems of a physical, chemical and technical nature, several strategies have been proposed to overcome the above issues, including the

selection of the appropriate liquid or stabilizing agent, the optimization of the focusing conditions and liquid levels, as well as the adoption of scanning and fluid dynamics strategies by different liquid handling configurations [41][42][43][44][45] and the postirradiation of colloids [46].

To explore the wide range of opportunities that LAL brings, the unique properties of femtosecond lasers is a further hot research topic, not only to increase NP production, but also to generate structural modifications and new material phases [47][48]. As reported by Streubel et al. [49], low productivity shortcomings in LAL have been almost entirely remedied, reaching NP production rates of several grams per hour. In addition to LAL, Laser Melting in Liquids (LML), Laser Fragmentation in Liquids (LFL) as well as pulsed Laser Photoreduction/oxidation in Liquids (LPL), offer alternative routes to obtain colloids with controlled NP sizes. Nevertheless, an industrial series product, or manufacturing process based on laser-synthesized particles is yet to come. Together with the development of new strategies to increase NP productivity, future efforts should be directed to further improve the surface properties of the produced NPs, since each application requires a different surface/interface chemistry. This would ensure reaching an advanced stage in those applications where the surface processes determine the performance of the final devices [50].

2. Promising Applications of LAL Nanostructures for Biotechnology Applications and for Organic Pollutants Degradation

2.1. Plasmonic Properties of Metal Nanoparticles and Plasmon Sensitivity

Plasmonics involves the control of light at the nanoscale by using surface plasmons. Localized surface plasmon resonance (LSPR), which imparts unique optical properties to metal nanostructures, involves the collective and coherent oscillation of dielectrically confined conduction electrons on the surface of metal nanostructures under the effect of electromagnetic fields [51][52].

Owing to the unique combination of physical and chemical properties, such as large absorption and scattering cross-section, high sensitivity to local dielectric environment and enhanced electric field at the surface, plasmonic nanostructures are emerging as an important class of materials for various optical sensing applications. Plasmonic systems in particular have been studied extensively due to their ability to confine light below the diffraction limit, which greatly enhances their sensitivity compared to conventional approaches [53]. The oscillating electric field of an electromagnetic wave causes the formation of dipoles and multipoles in metallic NPs. Such multipoles depend on the size and shape of the NP in a way predictable by solving the Maxwell equations at the interface between the metal and the external medium. For noble metals, the plasmonic response of the NP falls into the UV-vis frequency range and it is observed by considering the absorption and scattering cross sections. In a classical transmittance experiment the overall extinction effect (the sum of scattering and absorption) can be measured. If we restrict our consideration to a spherical NP with a size smaller than the excitation wavelength so that the impinging radiation wavelength scattering can be neglected (quasi static approximation) and a simple dipole is sufficient to account for the plasmonic behavior:

$$\mu = \alpha E$$

where α is the electric polarizability and E is the electric field. In this case the polarizability is expressed as:

where ϵ is the dielectric function [$\epsilon_1(\omega)+i\epsilon_2(\omega)$] and R the radius of the NP. The resonance condition is achieved for maximum polarizability, which happens for $\epsilon = -2\epsilon_m$. It is thus clear that plasmon resonance depends on the metal through its dielectric function and the NP size and on the medium through its dielectric constant ϵ_m (and thus the refractive index n). Much more complex is the situation in all those cases where the NP has a shape far from spherical-like and proper simulations about the plasmonic response should be conducted to interpret the response [51][53][54].

Laser ablation of metallic targets permits the formation of noble metal NPs in a range of solvents, including water and alcohols. Among noble metals, gold has been the most intensely studied, followed by silver. Both NPs can be produced as stable suspensions by LAL with diameters in the range 10–30 nm. Being different metals, they have different dielectric functions allowing plasmon resonances in different spectral regions. Indeed, Ag NPs have their typical plasmon resonance just below 400 nm, which instead lies around 510–530 nm for Au NPs. Despite plasmon resonance depending on particle size, a tuning across a broad range of the spectrum is not achievable just by adjusting spherical particle size. One way to overcome the issue is by alloying [54][55]. Figure 1a shows that even Au/Ag colloidal NP alloys can be grown if the ablation is performed using an alloy target in water [56]. Here, we refer to a gold 70% molar concentration with respect to silver, but any result can be obtained by tuning the concentration, thanks to the total miscibility of the two metals. This ensures the possibility to tune the plasmon resonance from that of silver (400 nm) to that of gold (520 nm) continuously, opening the

way to a fine plasmonic response. Alternatively, a very similar result can be obtained by pulsed laser irradiation of a previously formed Au/Ag colloidal mixture [56]. While in the former case the plasmon resonance tuning can be achieved only by choosing a different alloy target for every composition, in the latter case, the colloidal mixture can be prepared in any metal ratio from pure metal colloids, which is a clear advantage. Figure 1b reports a range of simulations conducted using a Boundary Element Method (BEM) developed by A. Trügler [57]. In this case a dielectric environment (water) where bodies with homogeneous and isotropic dielectric functions are separated by abrupt interfaces is assumed, thus solving Maxwell equations using the boundary conditions at the particle boundaries. As for the dielectric function of the considered Au/Ag alloy, a weighted average method was used, in which the dielectric function of the alloy is defined as:

$$\epsilon_{\text{alloy}}(\omega) = x \epsilon_{\text{Au}}(\omega) + (1 - x) \epsilon_{\text{Ag}}(\omega)$$

where x denotes the Au molar fraction in the Au–Ag alloy [58].

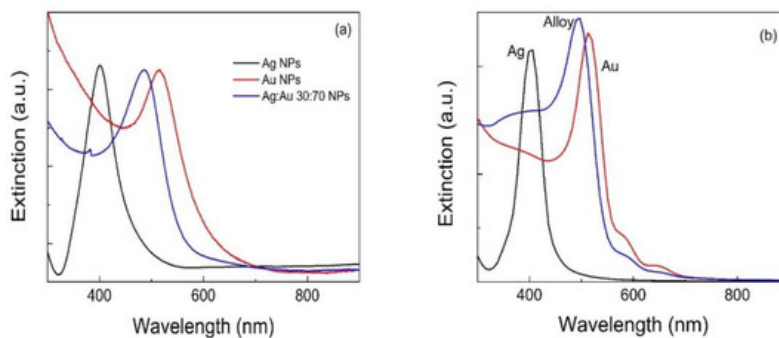


Figure 1. Absorption spectra of Ag, Ag:Au and Au NP colloids produced from: **(a)** laser ablation in liquids of Ag, Ag:Au alloy and Au targets, respectively; **(b)** a Boundary Element Method (BEM) simulation.

The simulation results shown in Figure 14b agree with the experimental results concerning the plasmon resonance position. The smaller width of the simulated extinction spectra is attributed to the difficulty to set an appropriate damping constant. The same BEM method predicts that as an Au NP grows larger, the plasmon resonance slightly red-shifts and broadens. However, in order to be able to tune the plasmon resonance of a metallic NP, playing with the size is not enough to explore a broad range [52][59]. Equation (1) holds its general validity for spherical particles, while for particles with different shapes, the geometry must be taken into account and a plasmon resonance shift can be expected. Indeed, beside the aforementioned alloying, a shape change is another effective strategy to tune the plasmon resonance. This was observed experimentally in gold nanorods [60][61], gold nanostars [62] and silver nanoplates [63][64].

2.2. Plasmonic Nanocolloids for Biotechnology Applications

Colloidal solutions of plasmonic NPs synthesized by laser ablation in solution (LAL) are key materials for biotechnology applications. We discuss some of our contributions to recall such applications. NPs are synthesized without stabilizing species, in order to avoid any associated biocompatibility problem. Furthermore, the naked surface of these NPs can be easily functionalized, for example with molecules for active cell targeting [65][66][67], for sensing and diagnosis [68][69][70], for drug monitoring [177] and also for therapies, as in the case of photothermal therapy [65][69]. Using multiple functionalizations, theranostic nanosystems, namely nanosystems useful for both therapy and diagnosis, can also be obtained.

Thanks to their chemical stability gold nanoparticles (AuNPs) are very frequently used in comparison to other metallic NPs, such as Ag NPs, which cause toxic effects due to ion solubilization. The presence of localized surface plasmons (LSPs) is an interesting property of this type of NPs that can be exploited for many applications. LSPs arise from collective oscillations of the free electrons of metal nanoparticles and show resonances in the visible and near infrared spectral range, depending on shape, dimensions and aggregation of the nanostructures, with very large extinction cross sections if compared to organic dyes [63]. LSP resonances (LSPR) depend also on the particle surrounding (in particular by its refractive index) and sensors can be developed on such a dependence. Moreover, excitation of the LSPR amplifies the incoming electromagnetic field at the NP surface by some orders of magnitudes within a few nm [71]. This amplification made possible the exploitation of Raman spectroscopy in the field of sensing technology with the technique called Surface Enhanced Raman Scattering (SERS). In this case, for molecules near the surface of plasmonic NPs, one can obtain amplifications of the vibrational Raman spectrum of up to 10 orders of magnitude and even more in favorable conditions [71].

NPs synthesized by LAL are of particular interest because of their clean surface, which allows functional molecules to reach easily the NP surface [72][73]. Antigen cell targeting [65][66][67][73][74][75], direct or indirect analytical sensors [76][72][77] and multimodal contrast agent in vivo [75] are examples of recent results obtained in our laboratories with plasmonic nanostructures for biotechnology applications.

The identification of antigens expressed by cells allows active targeting of individual cells, which is relevant in the early stage recognition of cancer cells. We developed a methodology for detecting cancer cells based on sub-nanomolar concentration of nanocolloids functionalized with monoclonal antibodies [56][57] or with engineered targeting peptides [66][73][74][75][77]. SERS labels, namely molecules showing huge SERS signals when coupled to plasmonic NPs, were used on the nanostructures to identify active targeting events using the presence of SERS signals on individual cells incubated with the nanostructures. SERS signals are vibrational signals, which are easily recognized and cannot be confused with other signals, like in the case of fluorescent signals usually exploited for this purpose. Our protocol is efficient because the naked particles, synthesized by laser ablation, are functionalized simply by mixing the colloidal solution of Au NPs with the solutions of the targeting molecules, without the need to control the exchange with stabilizing molecules used in other NP preparations. Molecules and also antibodies are thiolated to assure a strong link with the Au NPs. Strong SERS signals are obtained by controlling the aggregations of NPs, which create the hot spots where molecules show very intense SERS signals.

Incubations of the functionalized nanostructures were obtained with cancer cells overexpressing, or not, the target antigen. For the active targeting of prostatic cancer cells, nanostructures functionalized with antibodies for prostatic specific membrane antigen (PSMA) and prostate stem cell antigen (PSCA) antigens were considered [71][73]. Sensitivity (correct targeting among positive cells) and specificity (absence of targeting among negative cells) of the order of 90% were obtained showing the efficiency of the prepared nanostructures [73].

Monoclonal antibodies can be, however, immunogenic and usually their cost is very high. Small molecules like peptides are targeting units that do not show the problem of immunogenicity and their cost is much lower. In this case, however, the affinity for specific antigens is low. We have prepared nanostructures with the following peptides: GE11, which targets epidermal growth factor receptors (EGFRs) expressed in different types of tumors [66][74], RGD for v3 integrin, an adhesion receptor found in tumors at metastatic level [75], targeting and PreS1 for SerpinB3, a protein overexpressed by liver tumor cells, targeting [73].

The results show the need to engineer the peptides for the NP functionalization. A long polyethylene glycol (PEG) chain (3000 molecular weight) and a short-charged lysine sequence linked to the active peptide are required to obtain high targeting efficiencies that, in particular for specificity, are found to be better than those obtained with a specific monoclonal antibody already used in clinic. The results suggest that the large number of peptides (thousands per particle) per NP overcome the problem of the small affinity of the single peptide, exploiting the avidity of an ensemble of targeting units on a single nanostructure. With this approach, sensitivity and specificity larger than 80–90% are obtained [65][75] (see [Figure 2a](#)). Models for the arrangement of the targeting units on the Au NP surface, obtained with Molecular Dynamics calculations, show that the presence of the short lysine charged sequence is strategic for obtaining the appropriate exposition of the targeting peptide over the PEG chains, collapsed over the NP surface [66][75].

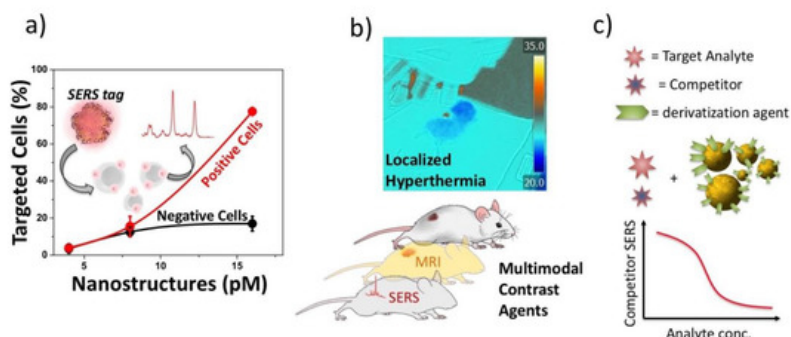


Figure 2. Nanoparticles obtained by LAL are particularly versatile for biotechnology applications. (a) active antigen targeting of cells overexpressing or not the antigen using Surface Enhanced Raman Scattering (SERS) signals; (b) multimodal contrast agents and hyperthermal experiments; (c) therapeutic drug monitoring with a competitive SERS protocol.

2.3. Metal Oxide Nanostructures for UV-SERS Sensing Applications

Traditionally, nanoplasmonics focuses on noble metals (Au, Ag, Cu) or their alloys whose LSPRs are in the visible (Vis) or near-infrared (NIR) spectral regions [78]. In the ultraviolet (UV) region the considerable damping due to interband transitions [79] make electromagnetic enhancements comparatively small. Nevertheless, UV nanoplasmonics may offer new opportunities in surface-enhanced Raman spectroscopy (SERS) [80], photocatalysis [81], biology [82] and public safety and security for the detection of organic molecules and hazardous organic compounds [83]. Such molecules show strong electronic absorption in the UV region, which may trigger the resonant Raman (RR) effect under UV excitation. The RR effect leads to ca. 10^8 -fold enhancement of the Raman cross-section, allowing to detect ultralow molecular concentrations [84].

Theoretical studies predict that metals with a large negative real part and a small imaginary part of the dielectric constant in the UV are suitable candidates for UV-SERS [85]. The most experimentally tested UV-SERS platforms are Al, Ga, In, Pb, Sn, Bi, Rh, Ru, Pt and Pd, owing to their availability and to the absence of interband transitions in the UV [86]. For instance, an ultrasensitive label-free detection of adenine molecules adsorbed on Al nanoparticle arrays using deep-UV SERS (with 257.2 nm excitation) was reported [87]. However, similar to Mg, Al suffers from the formation of an oxide layer several nanometers thick that limits the UV plasmonic performance. Although encapsulating the metal core within chemically inert ultrathin silica shells is a strategy to overcome this issue, it is difficult to implement given the not-easy-to-control thickness of the SiO₂ shell [88][89][90]. Ga is interesting for its self-terminating oxide monolayer, but it has an intrinsic low electrical conductivity besides the melting point near room temperature that hinders its manipulation [91][92]. Interestingly, Bi NPs prepared by laser ablation in solution [93] display LSPRs from the near UV to the IR absorption region. By using such Bi NPs as a SERS platform, the spectra of several amino acids were obtained [93], thus indicating that Bi could be considered an interesting material for the SERS detection of biomolecules, a task that is usually pursued by means of Ag and Au nanostructures. We outline that Bi plasmons lie in the UV region, whereas the Raman experiments were carried out with visible lasers [93], namely in correspondence of the tail of the optical absorption curve. Therefore, it is not possible to fully assess whether the Raman enhancement is purely electromagnetic, or chemical.

Among the transition metals, Rh has been recently discovered as a novel, nonoxidizing plasmonic contrast agent, exhibiting UV plasmonic behavior in the region between 3 eV and 7 eV, with the advantages of its oxide-free nature [94].

To date, the Rh nanostructures investigated were grown by electrochemical roughening of Rh surfaces [95] or by chemical methods using different Rh precursors [96][97][98][99]. The limited number of papers on UV-SERS is mainly because the application of deep-UV excitation very often leads to photo-degradation of the samples. The availability of a consistent SERS enhancement in the deep-UV spectral region would therefore allow recording Raman spectra with very low excitation power [84][97], which would be beneficial to reduce photo-degradation issues.

Under proper experimental conditions, LAL allows for the production of colloidal Rh suspensions in a suitable liquid medium [100][101][102], which can be employed for the fabrication of nanostructured Rh substrates with SPR peak in the 250–320 nm region. These LAL-synthesized Rh NPs are almost spherical, and their size and density distributions are markedly affected by the liquid (water, or ethanol) selected for LAL: Rh NPs obtained in water are smaller than those obtained in ethanol. The extinction spectra of the two colloids show the contribution associated to the SPR of the Rh NPs below 400 nm but, for the samples prepared in ethanol, an additional absorption feature is observed around 340 nm, which may be ascribed to Rh-C bonds [103]. The size of the NPs is affected by the chemical interactions that occur during the ablation process, in turn determined by the liquid environment. As discussed in [100], XRD and XPS results show that ablation of Rh in water leads to the production of mixed Rh/Rh-oxide phases (RhO₂ and Rh₂O₃), whereas in ethanol essentially metallic Rh NPs are produced, in agreement with [104].

By fabricating a simple conductometric platform with Rh NPs produced by LAL in water, Fazio et al. [100] have demonstrated the sensing properties of Rh nanostructures toward low concentration of hydrogen in air. Here, for the purpose of showing another potential application of Rh NPs produced by LAL in water, Fazio et al. report some early results on their SERS activity by considering the reference analyte Rhodamine 6G (R6G). By comparing the SERS spectrum of R6G on Rh NPs with the Raman spectrum acquired on bare glass under the same conditions (Figure 3a,b), the resulting enhancement factor is about 20, which shows the feasibility of using Rh NPs prepared by this technique as SERS substrates. The time-dependence of the SERS signal of R6G discloses the photo-induced degradation of the analyte adsorbed on the Rh/Rh-oxide NPs under the 457 nm laser irradiation (Figure 3c,d). Remarkably, a prompt and well-resolved SERS response is observed after just 3 s of irradiation. Then, after 110 s of irradiation, the strongest characteristic peak of R6G (1650 cm^{-1}) almost completely disappears (the same peak weakens by a factor of 0.4 after 22 s of irradiation). The photo-activity of nanostructured Rh surfaces was reported previously [105]; the data in Figure 3 parallel such behavior, which requires a careful control of irradiation conditions to use Rh-based NPs as a SERS

platform. LAL-synthesized Rh/Rh-oxide NPs arrays suitably arranged as thin films show a moderate SERS enhancement factor. Further optimizing the deposition conditions of the NPs is likely to improve the SERS performance of such substrates in the UV spectral region, which is of relevance for biological applications.

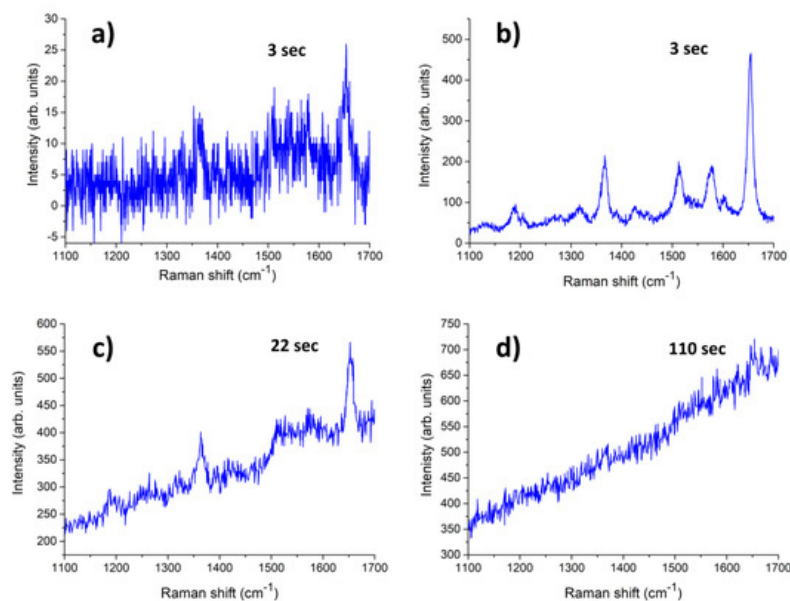


Figure 3. (a) Raman spectrum of R6G (10^{-4} M solution.) drop cast on glass and (b–d) Time-dependence of the SERS spectra of R6G (10^{-4} M solution) A drop of 10^{-4} M water solution of R6G was cast on the glass and dried in air before measurements; the Raman spectra were acquired using an HR800 micro-Raman spectrometer (Horiba, Jobin-Yvon, Longjumeau, France), using the 457.9 nm line of an Ar^+ ion laser, setting the laser power at 1 mW. The integration times were varied from a few seconds up to 110 s to maximize the signal to noise ratio.

References

1. Ealia, S.A.M.; Saravanakumar, M.P. A review on the classification, characterisation, synthesis of nanoparticles and their application. *IOP Conf. Ser. Mater. Sci. Eng.* 2017, 263, 032019.
2. Neri, G.; Fazio, E.; Mineo, P.G.; Scala, A.; Piperno, A. SERS Sensing Properties of New Graphene/Gold Nanocomposite. *Nanomaterials* 2019, 9, 1236.
3. Kuzmin, P.G.; Shafeev, G.A.; Bukin, V.V.; Garnov, S.V.; Farcau, C.; Carles, R.; Warot-Fontrose, B.; Guieu, V.; Viau, G. Silicon Nanoparticles Produced by Femtosecond Laser Ablation in Ethanol: Size Control, Structural Characterization, and Optical Properties. *J. Phys. Chem. C* 2010, 114, 15266–15273.
4. Szeffler, B. Nanotechnology, from quantum mechanical calculations up to drug delivery. *Int. J. Nanomed.* 2018, 13, 6143–6176.
5. Wolfsteller, A.; Geyer, N.; Nguyen-Duc, T.-K.; Das Kanungo, P.; Zakharov, N.; Reiche, M.; Erfurth, W.; Blumtritt, H.; Kalem, S.; Werner, P.; et al. Comparison of the top-down and bottom-up approach to fabricate nanowire-based silicon/germanium heterostructures. *Thin Solid Films* 2010, 518, 2555–2561.
6. Bera, D.; Qian, L.; Tseng, T.-K.; Holloway, P.H. Quantum Dots and Their Multimodal Applications: A Review. *Materials* 2010, 3, 2260–2345.
7. Damilano, B.; Coulon, P.-M.; Vézian, S.; Brändli, V.; Duboz, J.-Y.; Massies, J.; Shields, P.A. Top-down fabrication of GaN nano-laser arrays by displacement Talbot lithography and selective area sublimation. *Appl. Phys. Express* 2019, 12, 045007.
8. Fazio, E.; Scala, A.; Grimato, S.; Ridolfo, A.; Grassi, G.P.; Neri, F. Laser light triggered smart release of silibinin from a PEGylated–PLGA gold nanocomposite. *J. Mater. Chem. B* 2015, 3, 9023–9032.
9. Marco Bonelli; Antonio Miotello; Paolo M. Ossi; Alessandro Pessi; Stefano Gialanella; Laser-irradiation-induced structural changes on graphite. *Physical Review B* 1999, 59, 13513-13516, 10.1103/physrevb.59.13513.
10. Marcella Dell'aglio; Vincent Motto Ros; Frederic Pelascini; Igor B Gornushkin; Alessandro De Giacomo; Investigation on the material in the plasma phase by high temporally and spectrally resolved emission imaging during pulsed laser ablation in liquid (PLAL) for NPs production and consequent considerations on NPs formation. *Plasma Sources Science and Technology* 2019, 28, 085017, 10.1088/1361-6595/ab369b.

11. Petridis, C.; Savva, K.; Kymakis, E.; Stratakis, E. Laser generated nanoparticles based photovoltaics. *J. Colloid Interface Sci.* 2017, 489, 28–37.
12. Carter, M.J.; El-Desouky, A.; Andre, M.A.; Bardet, P.; Leblanc, S. Pulsed laser melting of bismuth telluride thermoelectric materials. *J. Manuf. Process.* 2019, 43, 35–46.
13. Zang, X.; Jian, C.; Zhu, T.; Fan, Z.; Wang, W.; Wei, M.; Li, B.; Diaz, M.F.; Ashby, P.; Lu, Z.; et al. Laser-sculptured ultrathin transition metal carbide layers for energy storage and energy harvesting applications. *Nat. Commun.* 2019, 10, 1–8.
14. Xie, B.; Wang, Y.; Lai, W.; Lin, W.; Lin, Z.; Zhang, Z.; Zou, P.; Xu, Y.; Zhou, S.; Yang, C.; et al. Laser-processed graphene based micro-supercapacitors for ultrathin, rollable, compact and designable energy storage components. *Nano Energy* 2016, 26, 276–285.
15. Picca, R.A.; Di Maria, A.; Riháková, L.; Volpe, A.; Sportelli, M.C.; Lugarà, P.M.; Ancona, A.; Cioffi, N. Laser Ablation Synthesis of Hybrid Copper/Silver Nanocolloids for Prospective Application as Nanoantimicrobial Agents for Food Packaging. *MRS Adv.* 2016, 1, 3735–3740.
16. Soman, P.; Zhang, W.; Umeda, A.; Zhang, Z.J.; Chen, S. Femtosecond laser-assisted optoporation for drug and gene delivery into single mammalian cells. *J. Biomed. Nanotechnol.* 2011, 7, 334–341.
17. Neri, G.; Corsaro, C.; Fazio, E. Plasmon-Enhanced Controlled Drug Release from Ag-PMA Capsules. *Molecules* 2020, 25, 2267–2278.
18. Tsuji, T.; Yahata, T.; Yasutomo, M.; Igawa, K.; Tsuji, M.; Ishikawa, Y.; Koshizaki, N. Preparation and investigation of the formation mechanism of submicron-sized spherical particles of gold using laser ablation and laser irradiation in liquids. *Phys. Chem. Chem. Phys.* 2013, 15, 3099–3107.
19. Kucherik, A.O.; Ryabchikov, Y.V.; Kutrovskaya, S.V.; Al-Kattan, A.; Arakelyan, S.M.; Itina, T.E.; Kabashin, A.V. Cavitation-Free Continuous-Wave Laser Ablation from a Solid Target to Synthesize Low-Size-Dispersed Gold Nanoparticles. *ChemPhysChem* 2017, 18, 1185–1191.
20. Mafuné, F.; Kohno, J.-Y.; Takeda, A.Y.; Kondow, T.; Sawabe, H. Formation of Gold Nanoparticles by Laser Ablation in Aqueous Solution of Surfactant. *J. Phys. Chem. B* 2001, 105, 5114–5120.
21. Besner, S.; Kabashin, A.V.; Winnik, F.M.; Meunier, M. Ultrafast laser based “green” synthesis of non-toxic nanoparticles in aqueous solutions. *Appl. Phys. A* 2008, 93, 955–959.
22. Pyatenko, A.; Wang, H.; Koshizaki, N.; Tsuji, T. Mechanism of pulse laser interaction with colloidal nanoparticles. *Laser Photon Rev.* 2013, 7, 596–604.
23. Jeevanandam, J.; Barhoum, A.; Chan, Y.S.; Dufresne, A.; Danquah, M.K. Review on nanoparticles and nanostructured materials: History, sources, toxicity and regulations. *Beilstein J. Nanotechnol.* 2018, 9, 1050–1074.
24. Zhang, D.; Gökce, B.; Barcikowski, S. Laser Synthesis and Processing of Colloids: Fundamentals and Applications. *Chem. Rev.* 2017, 117, 3990–4103.
25. Amendola, V.; Amans, D.; Ishikawa, Y.; Koshizaki, N.; Scirè, S.; Compagnini, G.; Reichenberger, S.; Barcikowski, S. Room-Temperature Laser Synthesis in Liquid of Oxide, Metal-Oxide Core-Shells, and Doped Oxide Nanoparticles. *Chem. Eur. J.* 2020, 26, 9206–9242.
26. Park, H.; Reddy, D.A.; Kim, Y.; Lee, S.; Ma, R.; Kim, T.K. Synthesis of Ultra-Small Palladium Nanoparticles Deposited on CdS Nanorods by Pulsed Laser Ablation in Liquid: Role of Metal Nanocrystal Size in the Photocatalytic Hydrogen Production. *Chem. Eur. J.* 2017, 23, 13112–13119.
27. Reichenberger, S.; Marzun, G.; Muhler, M.; Barcikowski, S. Perspective of Surfactant-Free Colloidal Nanoparticles in Heterogeneous Catalysis. *ChemCatChem* 2019, 11, 4489–4518.
28. Waag, F.; Li, Y.; Ziefuß, A.R.; Bertin, E.; Kamp, M.; Duppel, V.; Marzun, G.; Kienle, L.; Barcikowski, S.; Gökce, B. Kinetically-controlled laser-synthesis of colloidal high-entropy alloy nanoparticles. *RSC Adv.* 2019, 9, 18547–18558.
29. Lentini, G.; Fazio, E.; Calabrese, F.; De Plano, L.M.; Puliafico, M.; Franco, D.; Nicolò, M.S.; Carnazza, S.; Trusso, S.; Allegra, A.; et al. Phage–AgNPs complex as SERS probe for U937 cell identification. *Biosens. Bioelectron.* 2015, 74, 398–405.
30. Fazio, E.; Santoro, M.; Lentini, G.; Franco, D.; Guglielmino, S.P.P.; Neri, F. Iron oxide nanoparticles prepared by laser ablation: Synthesis, structural properties and antimicrobial activity. *Colloids Surf. A Physicochem. Eng. Asp.* 2016, 490, 98–103.
31. Tommasini, M.; Zanchi, C.; Lucotti, A.; Fazio, E.; Santoro, M.; Spadaro, S.; Neri, F.; Trusso, S.; Ciusani, E.; De Grazia, U.; et al. Laser synthesized nanoparticles for therapeutic drug monitoring. In *Advances in the Application of Lasers in Materials Science*; Ossi, P.M., Ed.; Springer: Cham, Switzerland, 2018; Volume 274, ISBN 978-3-319-96844-5.

32. Doñate-Buendía, C.; Frömel, F.; Wilms, M.B.; Streubel, R.; Tenkamp, J.; Hupfeld, T.; Nachev, M.; Gökce, E.; Weisheit, A.; Barcikowski, S.; et al. Oxide dispersion-strengthened alloys generated by laser metal deposition of laser-generated nanoparticle-metal powder composites. *Mater. Des.* 2018, 154, 360–369.
33. Hupfeld, T.; Wegner, A.; Blanke, M.; Doñate-Buendía, C.; Sharov, V.; Nieskens, S.; Piechotta, M.; Giese, M.; Barcikowski, S.; Gökce, B. Plasmonic Seasoning: Giving Color to Desktop Laser 3D Printed Polymers by Highly Dispersed Nanoparticles. *Adv. Opt. Mater.* 2020, 8, 2000473.
34. Fazio, E.; D'Urso, L.; Consiglio, G.; Giuffrida, A.; Compagnini, G.; Puglisi, O.; Patanè, S.; Neri, F.; Forte, G. Nonlinear Scattering and Absorption Effects in Size-Selected Diphenylpolyynes. *J. Phys. Chem. C* 2014, 118, 28812–28819.
35. Flores-Castañeda, M.; Camps, E.; Camacho-López, M.; Muhl, S.; García, E.; Figuero, M. Bismuth nanoparticles synthesized by laser ablation in lubricant oils for tribological tests. *J. Alloys Compd.* 2015, 643, S67–S70.
36. Torres-Mendieta, R. Fabrication of High Stable Gold Nanofluid by Pulsed Laser Ablation in Liquids. *Adv. Mater. Lett.* 2015, 6, 1037–1042.
37. Torres-Mendieta, R.; Mondragón, R.; Puerto-Belda, V.; Mendoza-Yero, O.; Lancis, J.; Juliá, J.E.; Mínguez-Vega, G. Characterization of Tin/Ethylene Glycol Solar Nanofluids Synthesized by Femtosecond Laser Radiation. *ChemPhysChem* 2017, 18, 1055–1060.
38. Rao, K.S.; Ganeev, R.A.; Zhang, K.; Fu, Y.; Boltaev, G.S.; Krishnendu, P.S.; Redkin, P.V.; Guo, C. Laser ablation-induced synthesis and nonlinear optical characterization of titanium and cobalt nanoparticles. *J. Nanoparticle Res.* 2018, 20, 285.
39. Fazio, E.; Neri, F.; Patanè, S.; D'Urso, L.; Compagnini, G. Optical limiting effects in linear carbon chains. *Carbon* 2011, 49, 306–310.
40. Zeng, H.; Du, X.; Guo, C.; Kulinich, S.; Yang, S.; He, J.; Cai, W. Nanomaterials via Laser Ablation/Irradiation in Liquid: A Review. *Adv. Funct. Mater.* 2012, 22, 1333–1353.
41. Wagener, P.; Barcikowski, S. Laser fragmentation of organic microparticles into colloidal nanoparticles in a free liquid jet. *Appl. Phys. A* 2010, 101, 435–439.
42. Amendola, V.; Polizzi, S.; Meneghetti, M. Free Silver Nanoparticles Synthesized by Laser Ablation in Organic Solvents and Their Easy Functionalization. *Langmuir* 2007, 23, 6766–6770.
43. Chemin, A.; Lam, J.; Laurens, G.; Trichard, F.; Motto-Ros, V.; LeDoux, G.; Jary, V.; Laguta, V.; Nikl, M.; Dujardin, C.; et al. Doping nanoparticles using pulsed laser ablation in a liquid containing the doping agent. *Nanoscale Adv.* 2019, 1, 3963–3972.
44. Streubel, R.; Barcikowski, S.; Gökce, B. Continuous multigram nanoparticle synthesis by high-power, high-repetition-rate ultrafast laser ablation in liquids. *Opt. Lett.* 2016, 41, 1486–1489.
45. Menéndez-Manjón, A.; Wagener, P.; Barcikowski, S. Transfer-Matrix Method for Efficient Ablation by Pulsed Laser Ablation and Nanoparticle Generation in Liquids. *J. Phys. Chem. C* 2011, 115, 5108–5114.
46. González-Rubio, G.; Guerrero-Martínez, A.; Liz-Marzán, L.M. Reshaping, Fragmentation, and Assembly of Gold Nanoparticles Assisted by Pulse Lasers. *Acc. Chem. Res.* 2016, 49, 678–686.
47. González-Rubio, G.; Díaz-Núñez, P.; Rivera, A.; Prada, A.; Tardajos, G.; González-Izquierdo, J.; Bañares, L.; Llombart, P.; MacDowell, L.G.; Palafox, M.A.; et al. Femtosecond laser reshaping yields gold nanorods with ultranarrow surface plasmon resonances. *Science* 2017, 358, 640–644.
48. Doñate-Buendía, C.; Fernández-Alonso, M.; Lancis, J.; Mínguez-Vega, G. Overcoming the barrier of nanoparticle production by femtosecond laser ablation in liquids using simultaneous spatial and temporal focusing. *Photon. Res.* 2019, 7, 1249–1257.
49. Streubel, R.; Bendt, G.; Gökce, B. Pilot-scale synthesis of metal nanoparticles by high-speed pulsed laser ablation in liquids. *Nanotechnology* 2016, 27, 205602.
50. Villa, M.D.A.; Gaudin, J.; Amans, D.; Boudjada, F.; Bozek, J.; Grisenti, R.E.; Lamour, E.; Laurens, G.; Macé, S.; Nicolas, C.; et al. Assessing the Surface Oxidation State of Free-Standing Gold Nanoparticles Produced by Laser Ablation. *Langmuir* 2019, 35, 11859–11871.
51. Stockman, M.I. Nanoplasmonics: Past, present, and glimpse into future. *Opt. Express* 2011, 19, 22029–22106.
52. Trugler, A. *Optical Properties of Metallic Nanoparticles*; Springer: Cham, Switzerland, 2016.
53. Gramotnev, D.K.; Bozhevolnyi, S.I. Plasmonics beyond the diffraction limit. *Nat. Photonics* 2010, 4, 83–91.
54. Fazio, E.; Saija, R.; Santoro, M.; Abir, S.; Neri, F.; Tommasini, M.; Ossi, P.M. On the Optical Properties of Ag–Au Colloidal Alloys Pulsed Laser Ablated in Liquid: Experiments and Theory. *J. Phys. Chem. C* 2020.

55. Lee, I.; Han, S.W.; Kim, K. Production of Au–Ag alloy nanoparticles by laser ablation of bulk alloys. *Chem. Commun.* 2001, 18, 1782–1783.
56. Compagnini, G.; Messina, E.; Puglisi, O.; Nicolosi, V. Laser synthesis of Au/Ag colloidal nano-alloys: Optical properties, structure and composition. *Appl. Surf. Sci.* 2007, 254, 1007–1011.
57. Waxenegger, J.; Trügler, A.; Hohenester, U. Plasmonics simulations with the MNPBEM toolbox: Consideration of substrates and layer structures. *Comput. Phys. Commun.* 2015, 193, 138–150.
58. Farokhnezhad, M.; Esmailzadeh, M. Optical and Photothermal Properties of Graphene Coated Au–Ag Hollow Nanoshells: A Modeling for Efficient Photothermal Therapy. *J. Phys. Chem. C* 2019, 123, 28907–28918.
59. Hohenester, U.; Trügler, A. MNPBEM—A Matlab toolbox for the simulation of plasmonic nanoparticles. *Comput. Phys. Commun.* 2012, 183, 370–381.
60. González-Rubio, G.; Kumar, V.; Lombart, P.; Díaz-Núñez, P.; Bladt, E.; Altantzis, T.; Bals, S.; Peña-Rodríguez, O.; Noya, E.G.; MacDowell, L.G.; et al. Disconnecting Symmetry Breaking from Seeded Growth for the Reproducible Synthesis of High Quality Gold Nanorods. *ACS Nano* 2019, 13, 4424–4435.
61. Attia, Y.A.; Flores-Arias, M.T.; Nieto, D.; Vázquez-Vázquez, C.; De La Fuente, G.F.; López-Quintela, M.A. Transformation of Gold Nanorods in Liquid Media Induced by nIR, Visible, and UV Laser Irradiation. *J. Phys. Chem. C* 2015, 119, 13343–13349.
62. Barbosa, S.; Agrawal, A.; Rodríguez-Lorenzo, L.; Pastoriza-Santos, I.; Alvarez-Puebla, R.A.; Kornowski, A.; Weller, H.; Liz-Marzán, M. Tuning Size and Sensing Properties in Colloidal Gold Nanostars. *Langmuir* 2010, 26, 14943–14950.
63. Hu, G.; Jin, W.; Zhang, W.; Wu, K.; He, J.; Zhang, Y.; Chen, Q.; Zhang, W. Surfactant-assisted shape separation from silver nanoparticles prepared by a seed-mediated method. *Colloids Surfaces A: Physicochem. Eng. Asp.* 2018, 540, 136–142.
64. Nguyen, T.H.N.; Nguyen, T.D.; Cao, M.T.; Van Viet, P. Fast and simple synthesis of triangular silver nanoparticles under the assistance of light. *Colloids Surfaces A: Physicochem. Eng. Asp.* 2020, 594, 124659.
65. Bertorelle, F.; Pinto, M.; Zappone, R.; Pilot, R.; Litt, L.; Fiameni, S.; Conti, G.; Gobbo, M.; Toffoli, G.; Colombatti, M.; et al. Safe core-satellite magneto-plasmonic nanostructures for efficient targeting and photothermal treatment of tumor cells. *Nanoscale* 2018, 10, 976–984.
66. Biscaglia, F.; Rajendran, S.; Conflitti, P.; Benna, C.; Sommaggio, R.; Litt, L.; Mocellin, S.; Bocchinfuso, G.; Rosato, A.; Palleschi, A.; et al. Enhanced EGFR Targeting Activity of Plasmonic Nanostructures with Engineered GE11 Peptide. *Adv. Heal. Mater.* 2017, 6, 1700596–1700604.
67. Meneghetti, M.; Scarsi, A.; Litt, L.; Marcolongo, G.; Amendola, V.; Gobbo, M.; Di Chio, M.; Boscaini, A.; Fracasso, G.; Colombatti, M. Plasmonic Nanostructures for SERRS Multiplexed Identification of Tumor-Associated Antigens. *Small* 2012, 8, 3733–3738.
68. Calzavara, D.; Ferraro, D.; Litt, L.; Cappozzo, G.; Mistura, G.; Meneghetti, M.; Pierno, M. Single File Flow of Biomimetic Beads for Continuous SERS Recording in a Microfluidic Device. *Adv. Condens. Matter Phys.* 2018, 2018, 1–9.
69. Litt, L.; Rivato, N.; Fracasso, G.; Bontempi, P.; Nicolato, E.; Marzola, P.; Venzo, A.; Colombatti, M.; Gobbo, M.; Meneghetti, M. A SERRS/MRI multimodal contrast agent based on naked Au nanoparticles functionalized with a Gd(III) loaded PEG polymer for tumor imaging and localized hyperthermia. *Nanoscale* 2018, 10, 1272–1278.
70. Del Tedesco, A.; Piotto, V.; Sponchia, G.; Hossain, K.; Litt, L.; Peddis, D.; Scarso, A.; Meneghetti, M.; Benedetti, A.; Riello, P. Zirconia-Based Magnetoplasmonic Nanocomposites: A New Nanotool for Magnetic-Guided Separations with SERS Identification. *ACS Appl. Nano Mater.* 2020, 3, 1232–1241.
71. Litt, L.; Meneghetti, M. Predictions on the SERS enhancement factor of gold nanosphere aggregate samples. *Phys. Chem. Chem. Phys.* 2019, 21, 15515–15522.
72. Fornasaro, S.; Alsamad, F.; Baia, M.; De Carvalho, L.A.E.B.; Beleites, C.; Byrne, H.J.; Chiadò, A.; Chis, M.; Chisanga, M.; Daniel, A.; et al. Surface Enhanced Raman Spectroscopy for Quantitative Analysis: Results of a Large-Scale European Multi-Instrument Interlaboratory Study. *Anal. Chem.* 2020, 92, 4053–4064.
73. Biscaglia, F.; Quarta, S.; Villano, G.; Turato, C.; Biasiolo, A.; Litt, L.; Ruzzene, M.; Meneghetti, M.; Pontisso, P.; Gobbo, M. PreS1 peptide-functionalized gold nanostructures with SERRS tags for efficient liver cancer cell targeting. *Mater. Sci. Eng. C* 2019, 103, 109762–109770.
74. Mazzuca, C.; Di Napoli, B.; Biscaglia, F.; Ripani, G.; Rajendran, S.; Braga, A.; Benna, C.; Mocellin, S.; Gobbo, M.; Meneghetti, M.; et al. Understanding the good and poor cell targeting activity of gold nanostructures functionalized with molecular units for the epidermal growth factor receptor. *Nanoscale Adv.* 2019, 1, 1970–1979.

75. Biscaglia, F.; Ripani, G.; Rajendran, S.; Benna, C.; Mocellin, S.; Bocchinfuso, G.; Meneghetti, M.; Palleschi, A.; Gobbo, M. Gold Nanoparticle Aggregates Functionalized with Cyclic RGD Peptides for Targeting and Imaging of Colorectal Cancer Cells. *ACS Appl. Nano Mater.* 2019, 2, 6436–6444.
76. Litti, L.; Ramundo, A.; Biscaglia, F.; Toffoli, G.; Gobbo, M.; Meneghetti, M. A surface enhanced Raman scattering based colloid nanosensor for developing therapeutic drug monitoring. *J. Colloid Interface Sci.* 2019, 533, 621–626.
77. Prati, S.; Quaranta, M.; Sciutto, G.; Bonacini, I.; Litti, L.; Meneghetti, M.; Mazzeo, R. Use of nano gold obtained by laser ablation for SEIRA analyses of colorants. *Herit. Sci.* 2014, 2, 1–12.
78. Chakravadhanula, V.S.K.; Mishra, Y.K.; Kotnur, V.G.; Avasthi, D.K.; Strunskus, T.; Zaporotchenko, V.; Fink, D.; Kienle, L.; Faupel, F. Microstructural and plasmonic modifications in Ag–TiO₂ and Au–TiO₂ nanocomposites through ion beam irradiation. *Beilstein J. Nanotechnol.* 2014, 5, 1419–1431.
79. Ahmadivand, A.; Sinha, R.; Kaya, S.; Pala, N. Rhodium plasmonics for deep-ultraviolet bio-chemical sensing. *Plasmonics* 2016, 11, 839–849.
80. Yang, Y.; Callahan, J.M.; Kim, T.-H.; Brown, A.S.; Everitt, H.O. Ultraviolet Nanoplasmonics: A Demonstration of Surface-Enhanced Raman Spectroscopy, Fluorescence, and Photodegradation Using Gallium Nanoparticles. *Nano Lett.* 2013, 13, 2837–2841.
81. Zhang, C.; Zhao, H.; Zhou, L.; Schlather, A.E.; Dong, L.; McClain, M.J.; Swearer, D.F.; Nordlander, P.; Halas, N.J. Al–Pd Nanodisk Heterodimers as Antenna–Reactor Photocatalysts. *Nano Lett.* 2016, 16, 6677–6682.
82. Anker, J.N.; Hall, W.P.; Lyandres, O.; Shah, N.C.; Zhao, J.; Van Duyne, R.P. Biosensing with plasmonic nanosensors. *Nanosci. Technol.* 2009, 308–319.
83. Kumamoto, Y.; Taguchi, A.; Honda, M.; Watanabe, K.; Saito, Y.; Kawata, S. Indium for Deep-Ultraviolet Surface-Enhanced Resonance Raman Scattering. *ACS Photon.* 2014, 1, 598–603.
84. Dörfer, T.; Schmitt, M.; Popp, J. Deep-UV surface-enhanced Raman scattering. *J. Raman Spectrosc.* 2007, 38, 1379–1382.
85. McMahon, J.M.; Schatz, G.C.; Gray, S.K. Plasmonics in the ultraviolet with the poor metals Al, Ga, In, Sn, Tl, Pb, and Bi. *Phys. Chem. Chem. Phys.* 2013, 15, 5415–5423.
86. Knight, M.W.; King, N.S.; Liu, L.; Everitt, H.O.; Nordlander, P.; Halas, N.J. Aluminum for Plasmonics. *ACS Nano* 2014, 8, 834–840.
87. Jha, S.K.; Ekinci, Y.; Agio, M.; Löffler, J.F. Towards deep-UV surface-enhanced resonance Raman spectroscopy of explosives: Ultrasensitive, real-time and reproducible detection of TNT. *Analyst* 2015, 140, 5671–5677.
88. Gutierrez, Y.; Ortiz, D.; Sanz, J.M.; Saiz, J.M.; Gonzalez, F.; Everitt, H.O.; Moreno, F. How an oxide shell affects the ultraviolet plasmonic behavior of Ga, Mg, and Al nanostructures. *Opt. Express* 2016, 24, 20621–20631.
89. Li, J.F.; Huang, Y.F.; Ding, Y.; Yang, Z.L.; Li, S.B.; Zhou, X.S.; Fan, F.R.; Zhang, W.; Zhou, Z.Y.; Wu, D.Y.; et al. Shell-isolated nanoparticle-enhanced Raman spectroscopy. *Nature* 2010, 464, 392–395.
90. Sterl, F.; Strohfeldt, N.; Walter, R.; Griessen, R.; Tittel, A.; Giessen, H. Magnesium as Novel Material for Active Plasmonics in the Visible Wavelength Range. *Nano Lett.* 2015, 15, 7949–7955.
91. Losurdo, M.; Suvorova, A.; Rubanov, S.; Hingerl, K.; Brown, A.S. Thermally stable coexistence of liquid and solid phases in gallium nanoparticles. *Nat. Mater.* 2016, 15, 995–1002.
92. Knight, M.W.; Coenen, T.; Yang, Y.; Brenny, B.J.M.; Losurdo, M.; Brown, A.S.; Everitt, H.O.; Polman, A. Gallium Plasmonics: Deep Subwavelength Spectroscopic Imaging of Single and Interacting Gallium Nanoparticles. *ACS Nano* 2015, 9, 2049–2060.
93. Bezerra, A.G.; Cavassin, P.; Machado, T.N.; Woiski, T.D.; Caetano, R.; Schreiner, W.H. Surface-enhanced Raman scattering using bismuth nanoparticles: A study with amino acids. *J. Nanopart. Res.* 2017, 19, 362.
94. Xie, S.; Liu, X.Y.; Xia, Y. Shape-controlled syntheses of rhodium nanocrystals for the enhancement of their catalytic properties. *Nano Res.* 2015, 8, 82–96.
95. Tian, N.; Zhou, Z.Y.; Sun, S.G.; Cui, L.; Ren, B.; Tian, Z.Q. Electrochemical preparation of platinum nanothorn assemblies with high surface enhanced Raman scattering activity. *Chem. Commun.* 2006, 39, 4090–4092.
96. Humphrey, S.M.; Grass, M.E.; Habas, S.E.; Niesz, K.; Somorjai, G.A.; Don Tilley, T. Rhodium nanoparticles from cluster seeds: Control of size and shape by precursor addition rate. *Nano Lett.* 2007, 7, 785–790.
97. Das, R.; Soni, R.K. Rhodium nanocubes and nanotriangles for highly sensitive ultraviolet surface-enhanced Raman spectroscopy. *Analyst* 2018, 143, 2310–2322.

98. Passoni, M.; Dellasega, D.; Grosso, G.; Conti, C.; Ubaldi, M.; Bottani, C.E. Nanostructured rhodium films produced by pulsed laser deposition for nuclear fusion applications. *J. Nucl. Mater.* 2010, 404, 1–5.
99. Uccello, A.; Dellasega, D.; Perissinotto, S.; Lecis, N.; Passoni, M. Nanostructured rhodium films for advanced mirrors produced by Pulsed Laser Deposition. *J. Nucl. Mater.* 2013, 432, 261–265.
100. Fazio, E.; Leonardi, S.; Santoro, M.; Donato, N.; Neri, G.; Neri, F. Synthesis, characterization and hydrogen sensing properties of nanosized colloidal rhodium oxides prepared by Pulsed Laser Ablation in water. *Sens. Actuators B: Chem.* 2018, 262, 79–85.
101. Santoro, M.; Fazio, E.; Trusso, S.; Ossi, P.M.; Tommasini, M.; Neri, F. Rhodium nanoparticles synthesized by nanosecond and picosecond Pulsed Laser Ablation in Liquid. GISR2016. In Proceedings of the Italian Meeting on Raman Spectroscopy and Non Linear Optic Effects, Padova, Italy, 14–16 September 2016.
102. Santoro, M.; Bertoncini, A.; Fazio, E.; Tommasini, M.; Neri, F.; Ossi, P.M.; Trusso, S. Nanostructured Rhodium Thin Films Deposited by Pulsed Laser Deposition for SERS Detection. CNS2018—4°. In Proceedings of the Congresso Nazionale Sensori, Catania, Italy, 21–23 February 2018.
103. Borodko, Y.; Sook Lee, H.; Joo, S.H.; Zhang, Y.; Somorjai, G. Spectroscopic Study of the Thermal Degradation of PVP-Capped Rh and Pt Nanoparticles in H₂ and O₂ Environments. *J. Phys. Chem. C* 2010, 114, 1117–1126.
104. Kato, K.; Abe, T.; Kawamura, M.; Sasaki, M. Preparation of RhO₂ Thin Films by Reactive Sputtering and Their Characterizations. *Jpn. J. Appl. Phys.* 2001, 40, 2399.
105. Li, A.; Lin, J.; Huang, Z.; Wang, X.; Guo, L. Surface-Enhanced Raman Spectroscopy on Amorphous Semiconducting Rhodium Sulfide Microbowl Substrates. *iScience* 2018, 10, 1–10.

Retrieved from <https://encyclopedia.pub/entry/history/show/17343>